

A wide-binary solar companion as a possible origin of Sedna-like objects

John J. Matese¹, Daniel P. Whitmire¹ and Jack J. Lissauer²

¹Department of Physics, University of Louisiana, Lafayette, LA, 70504-4210, USA
email: matese@louisiana.edu

²Space Science and Astrobiology Division, MS 245-3, NASA Ames Research Center,
Moffett Field, CA, 94035, USA

Abstract. Sedna is the first inner Oort cloud object to be discovered. Its dynamical origin remains unclear, and a possible mechanism is considered here. We investigate the parameter space of a hypothetical solar companion which could adiabatically detach the perihelion of a Neptune dominated TNO with a Sedna-like semimajor axis. Demanding that the TNO's maximum value of osculating perihelion exceed Sedna's observed value of 76 AU, we find that the companion's mass and orbital parameters (m_c, a_c, q_c, Q_c, i_c) are restricted to

$$m_c \gtrsim 5 M_J \left(\frac{Q_c}{7850 \text{ AU}} \frac{q_c}{7850 \text{ AU}} \right)^{3/2}$$

during the epoch of strongest perturbations. The ecliptic inclination of the companion should be in the range $45^\circ \lesssim i_c \lesssim 135^\circ$ if the TNO is to retain a small inclination while its perihelion is increased. We also consider the circumstances where the minimum value of osculating perihelion would pass the object to the dynamical dominance of Saturn and Jupiter, if allowed. It has previously been argued that an overpopulated band of outer Oort cloud comets with an anomalous distribution of orbital elements could be produced by a solar companion with present parameter values

$$m_c \approx 5 M_J \left(\frac{9000 \text{ AU}}{a_c} \right)^{1/2}.$$

If the same hypothetical object is responsible for both observations, then it is likely recorded in the IRAS and possibly the 2MASS databases.

Keywords. Kuiper Belt, Oort Cloud, comets:2003 VB₁₂, comets:general, binaries:general

1. Introduction

Brown, Trujillo & Rabinowicz (2004) have discovered the first inner Oort cloud object, Sedna (2003 VB₁₂) with a semimajor axis of $a = 489$ AU. Morbidelli and Levison (2004) consider various scenarios for a TNO origin of the detached orbit of Sedna-like objects (hereafter referred to as STNO). These outer STNO have been described by Emel'yanenko, Asher and Bailey (2002) and could not have been put into their present orbit by Neptune in its present orbit or by the galactic tide. Gomes *et al.* (2005) discuss two resonant mechanisms for converting objects in the scattered disk into high-perihelion ($q > 40$ AU) scattered disk objects, but they find that they cannot produce these detached objects with $a > 260$ AU. Morbidelli and Levison (2004) consider, and reject, three additional mechanisms, (i) the passage of Neptune through a high-eccentricity stage, (ii) the past existence of massive planetary embryos in the Kuiper belt or scattered disk, and (iii) the presence of a massive trans-Neptunian disk at early epochs which exerted tides on scattered disk objects. The only options which they find to give satisfactory results

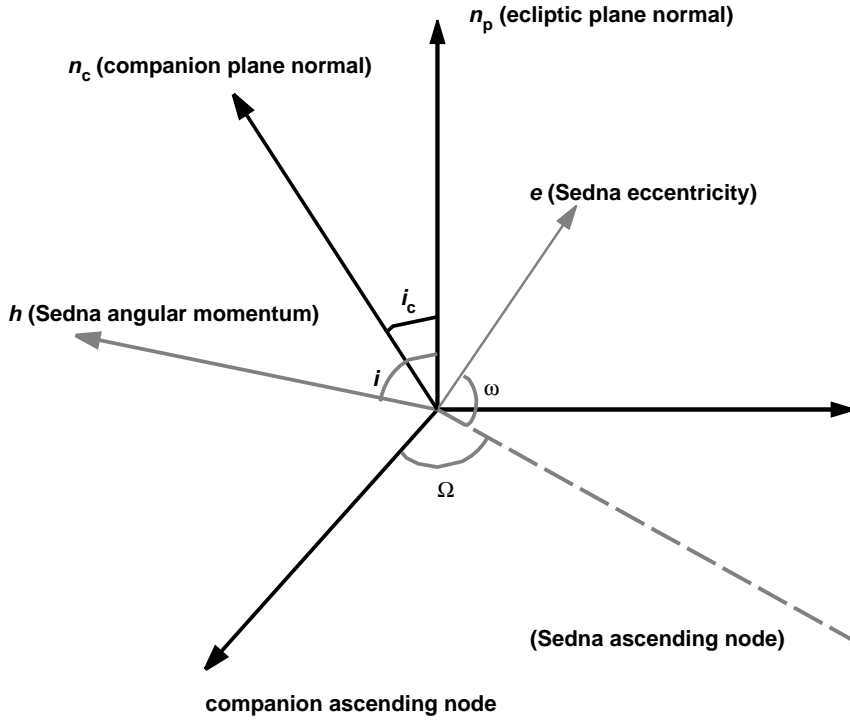


Figure 1. Orientation definitions of the orbital vectors.

are the passage of a low-velocity solar-mass star at about 800 AU during the early solar environment, or the capture of extrasolar planetesimals from a low-mass star or brown dwarf encountering the Sun. They observe that creating these “extended scattered disk objects” (in which the largest orbits also have the largest perihelia) requires a perturbation “from the outside”, but do not discuss the possibility that the external perturbation could come from a planetary-mass wide-binary solar companion. We consider that option here. Our goal is to limit the possible parameter space of a hypothetical solar companion which would be capable of detaching the orbit of an STNO from the dominance of Neptune. We further compare it to the parameter space of a hypothetical companion that has previously been suggested by an analysis of an overpopulated band of new Oort cloud comets with an anomalous distribution of orbital elements (Matese, Whitman and Whitmire (1999), Matese and Lissauer (2002)). Sec. 2 describes the dynamical analysis used. A discussion of some of the results is found in Sec. 3. We give our conclusions and summarize in Sec. 4.

2. Analysis

Our approach is detailed in the Appendix. We consider the equations of motion of the eccentricity vector and the angular momentum vector (see figure 1) of the STNO. The perturbations of the known planets (M_p, r_p) and a hypothetical wide-binary solar companion are included in a secularly averaged manner, with possible resonances and impulsive interactions being ignored. The companion interaction can then be characterized by only two parameters, its ecliptic inclination i_c and a dimensionless strength parameter,

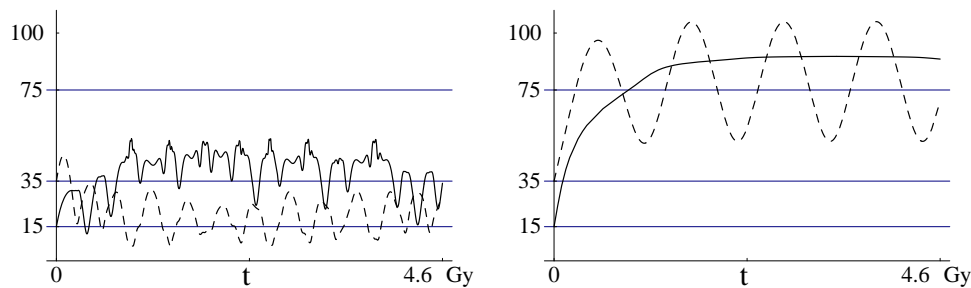


Figure 2. Some example calculations of the STNO osculating perihelion distance, q (AU) (dashed line) and inclination, i ($^\circ$) (solid line). i_c is the inclination of the companion orbit. γ_c is the ratio of the timescale for planetary perturbations divided by the timescale for companion perturbations. Ω_o and ω_o are, respectively, the initial values of the STNO longitude of ascending node and the STNO argument of perihelion. (left): $i_c = 60^\circ$, $\gamma_c = 10$, $\Omega_o = 100^\circ$, $\omega_o = 10^\circ$. (right): $i_c = 30^\circ$, $\gamma_c = 10$, $\Omega_o = 100^\circ$, $\omega_o = 10^\circ$.

γ_c , which is the ratio of the timescale for the adiabatic planetary perturbations divided by the timescale for the companion perturbation

$$\gamma_c \equiv \frac{2m_c a^5}{\sum_p (M_p r_p^2) \sqrt{q_c^3 Q_c^3}} \xrightarrow{\text{Sedna}} \frac{m_c}{M_J} \left(\frac{7850 \text{ AU}}{q_c} \frac{7850 \text{ AU}}{Q_c} \right)^{3/2}. \quad (2.1)$$

In the secular approximation, the semimajor axis of the STNO is taken to be constant at Sedna's present value of $a = 489$ AU and the remaining orbital elements i, ω, Ω and e are changed by the combined perturbations. We assume that each possible progenitor orbit of the STNO was dominated by Neptune with initial values $q_o = 35$ AU, $i_o = 15^\circ$. Sedna's present elements are $q = 76$ AU and $i = 11.9^\circ$. The remaining two initial elements of the token orbits, Ω_o, ω_o , are densely sampled over their ranges $0 \leftrightarrow 360^\circ$. We then integrate the equations over 4.6 Gy and record the maximum and minimum osculating perihelion distance, q_{max} and q_{min} and also record the inclination, i at q_{max} .

3. Results

The orbital variations can be categorized depending on the answers to the following questions: Does the maximum perihelion distance exceed the observed value of Sedna? Does the minimum perihelion distance enter the Saturn zone (where impulses can rapidly change the energy of the STNO)? Does the ecliptic inclination get driven to large values when the perihelion distance is increased beyond 76 AU? We choose a variety of companion parameter sets, i_c and γ_c , as well as initial STNO parameters, Ω_o and ω_o , to illustrate these three different characteristics of the osculating orbits. Circumstances where the nonlinear equations exhibit chaotic behavior can also be inferred.

3.1. Examples of Individual Calculations

Some example calculations of the complete time dependence of the osculating parameters are shown in figures 2, 3, 4. In figure 2, we compare two cases where the initial STNO orbit is the same, the companion strength parameter, γ_c , is the same, but the companion inclination, i_c , is different. We reject both of these possible detachment scenarios, but for different reasons. In figure 2l, the perihelion never detaches, while in figure 2r it does detach, but i is driven toward 90° .

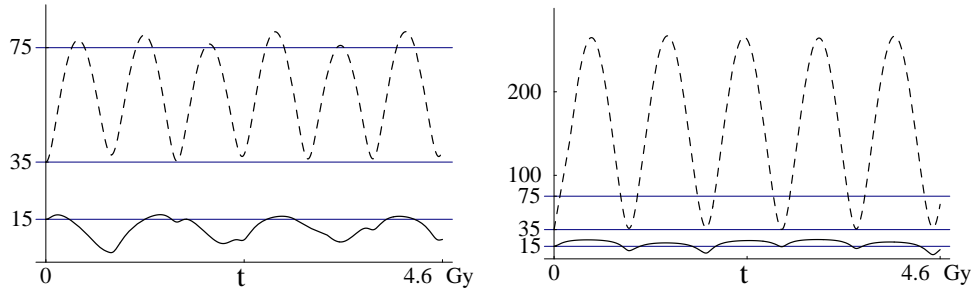


Figure 3. As in figure 2. (*left*): $i_c = 60^\circ$, $\gamma_c = 5$, $\Omega_o = 180^\circ$, $\omega_o = 180^\circ$.
(*right*): $i_c = 60^\circ$, $\gamma_c = 20$, $\Omega_o = 180^\circ$, $\omega_o = 180^\circ$.

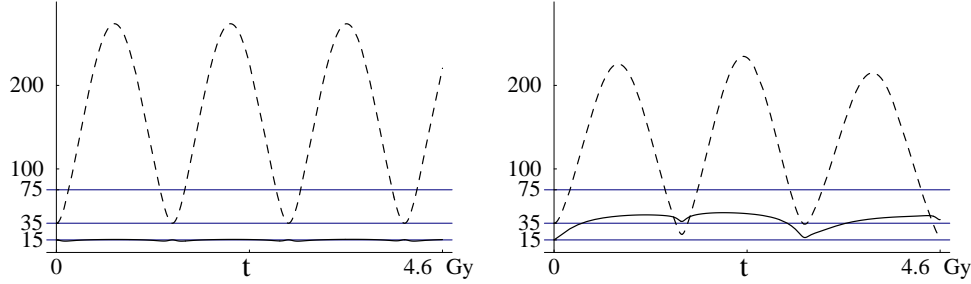


Figure 4. As in figure 2. (*left*): $i_c = 90^\circ$, $\gamma_c = 10$, $\Omega_o = 180^\circ$, $\omega_o = 180^\circ$.
(*right*): $i_c = 30^\circ$, $\gamma_c = 10$, $\Omega_o = 180^\circ$, $\omega_o = 180^\circ$.

Figure 3 contrasts two cases, again with identical initial STNO orbits, but now we maintain the same i_c and change γ_c . In figure 3*l*, the perihelion is detached to just beyond 75 AU, while in figure 3*r* it easily exceeds Sedna's present q . In both cases q_{min} remains beyond Neptune's orbit, and i remains small.

Finally, we show another pair of examples where only i_c is changed. In both cases acceptable values of q_{max} and q_{min} are obtained, but figure 4*l* shows a small i , while figure 4*r* shows a large i .

In order to infer global implications about the phase space of a hypothetical companion that could potentially produce an acceptable detached STNO orbit (without producing large i or small q_{min}), we present the results in a way that can be more readily synopsized.

3.2. Overview for Specific Companion Parameters

Surface and/or contour graphs of q_{max} , q_{min} and $i_{q_{max}}$ have been created for many specific sets of companion parameters, i_c , γ_c , distributed over all Ω_o, ω_o . In figure 5, we show these for companion parameters $i_c = 90^\circ$, $\gamma_c = 10$. We see that there is a significant region of (Ω_o, ω_o) phase space where $q_{max} \geq 76$ AU and $i_{q_{max}}$ remains small. For this case, $q_{min} > 15$ AU for all Ω_o, ω_o .

Figure 6 shows results for $i_c = 30^\circ$, $\gamma_c = 10$. We see here that there is no region of Ω_o, ω_o phase space where acceptable conditions for producing a STNO occur. Several specific cases shown in figures 2, 3, 4 can be found in the synopsized figures 5, 6.

A common feature of all parameter sets is that q_{max} tends to depend mainly on the

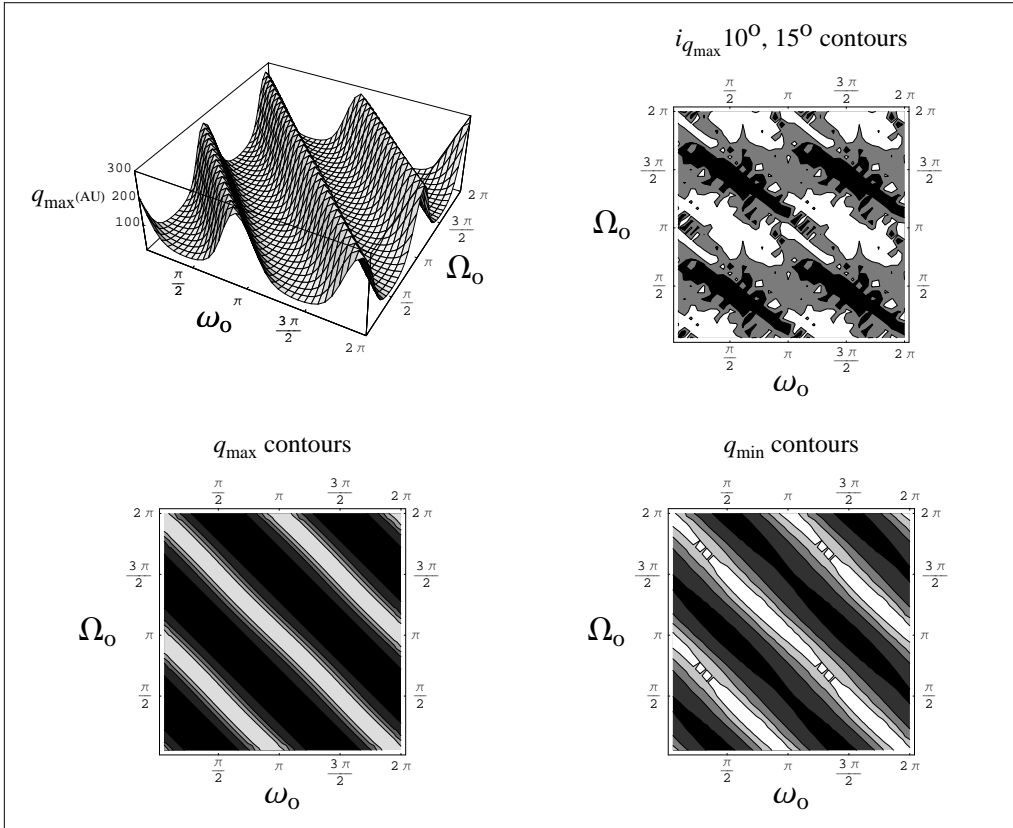


Figure 5. Summarizing results for companion parameters $i_c = 90^\circ$, $\gamma_c = 10$, over all initial STNO parameters Ω_o , ω_o . (*upper left*): surface plot of q_{max} . (*lower left*): contour plot with the region $q_{max} < 76$ AU shown in black. (*upper right*): contour plot of $i_{q_{max}}$ with the region $< 10^\circ$ shown in black and the region $> 15^\circ$ shown in white. (*lower right*): contour plot of q_{min} with the region $15 \text{ AU} < q_{min} < 18 \text{ AU}$ shown in black and $q_{min} \geq 35 \text{ AU}$ shown in white.

sum $\tilde{\omega}_o \equiv \Omega_o + \omega_o$ and peaks at $\tilde{\omega}_o \approx$ integer multiples of π (for the orientation chosen in figure 1). This is because of the small initial STNO inclination, $i_o = 15^\circ$.

4. Conclusions and Summary

We find that in the secular approximation, a solar companion strength parameter $\gamma_c \lesssim 5$ would not be able to detach a Sedna-like TNO to 76 AU, independent of its inclination, i_c , or of the initial STNO elements Ω_o , ω_o . If $\gamma_c \gtrsim 5$ there will always be some portion of the (Ω_o, ω_o) phase space where detachment to $q_{max} \geq 76$ AU can occur. However, if i_c is too small we find that detachment coincides with large STNO inclination, i . Summarizing, from Eq. 2.1 we see that the requirements for a hypothetical wide-binary solar companion to produce a STNO are

$$m_c \gtrsim 5 M_J \left(\frac{Q_c}{7850 \text{ AU}} \frac{q_c}{7850 \text{ AU}} \right)^{3/2}, \quad (4.1)$$

with $i_c \approx 90^\circ \pm 45^\circ$, during the epoch when γ_c was largest. Although Eq. 4.1 is scaled to M_J , we note that a Neptunian-mass companion at orbit distances $\gtrsim 2000$ AU could also detach a STNO and produce Sedna.

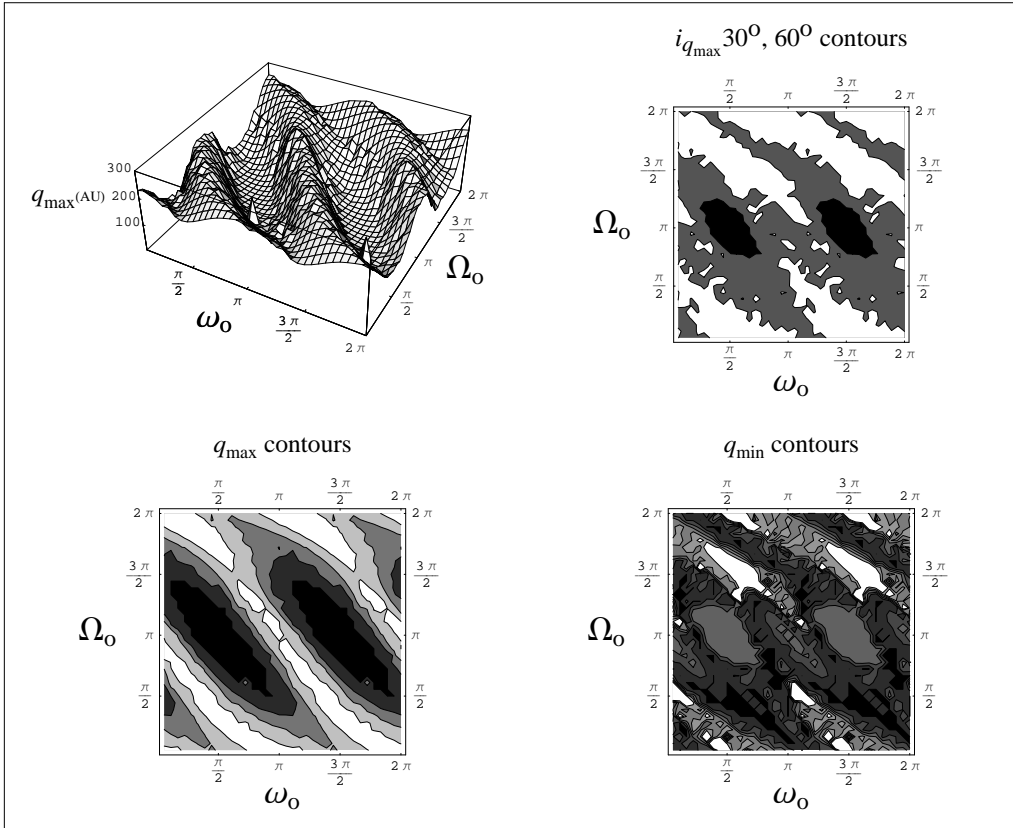


Figure 6. Summarizing results for companion parameters $i_c = 30^\circ$, $\gamma_c = 10$, over all initial STNO parameters Ω_o , ω_o . (*upper left*): surface plot of q_{max} . (*lower left*): contour plot with the region $q_{max} < 76$ AU shown in black. (*upper right*): contour plot of $i_{q_{max}}$ with the region $< 30^\circ$ shown in black. (*lower right*): contour plot of q_{min} with the region $q_{min} < 10$ AU shown in black and $q_{min} \geq 35$ AU shown in white.

The above limits have largely been confirmed in a more precise dynamical simulation which includes the hypothetical companion and the giant planets as particles and numerically integrates perturbations on a sampling that is based on the real population of scattered disk objects (Gomes, Matese and Lissauer (2006)). A substantive difference is that they find that Neptune provides an efficient mechanism for slowly pumping up a STNO semimajor axis if the companion reduces q and re-attaches the perihelion to Neptune dominance. However the timescale for companion induced detachment is typically shorter than the timescale for energy pumping by Neptune when $\gamma_c \gtrsim 5$.

A similar analysis has been performed for 2000 CR₁₀₅ which has $a = 221$ AU and $q = 44$ AU. We find that in this case detaching 2000 CR₁₀₅ requires a much closer companion,

$$m_c \gtrsim 5 M_J \left(\frac{Q_c}{4250 \text{ AU}} \frac{q_c}{4250 \text{ AU}} \right)^{3/2}, \quad (4.2)$$

with $i_c \approx 90^\circ \pm 60^\circ$. It is more likely that the explanation for detaching objects such as 2000 CR₁₀₅ lies in a resonant interaction (Gomes *et al.* (2005)).

These results can be compared to the claim (Matese, Whitman and Whitmire (1999), Matese and Lissauer (2002)) that a concentration of observed outer Oort cloud cometary

perihelia having an anomalous distribution of orbital elements could be due to a wide-binary companion with *present* parameters satisfying (to within a factor of 2)

$$m_c \approx 5 M_J \left(\frac{9000 \text{ AU}}{a_c} \right)^{1/2}. \quad (4.3)$$

The observational absence of a similar anomalous population of inner Oort cloud comets implies that any proposed companion presently in the inner Oort cloud region would have largely cleared out the inner Oort cloud phase space accessible to its impulses during the Solar System lifetime. Galactic tides and weak stellar impulses tend to randomize the outer Oort cloud phase space over timescales that are short compared to the depletion timescale of the hypothetical companion.

In figure 7, we graphically show these parameter ranges. Also shown are the limits for J-band ($\approx 1.2 \mu\text{m}$) observability in the 2MASS database and for unconfused sky observability in the IRAS $12 \mu\text{m}$ band (Burrows, Sudarsky & Lunine (2003)). A solar companion capable of both detaching Sedna and creating the Oort cloud anomaly would likely have been seen in the IRAS survey. Even if the hypothetical object has been recorded in these databases, it is unlikely to have been perceived as a solar companion.

The recent discovery of the 2MASS binary 2M1207a,b (Chauvin, *et al.* (2004)) in which a $5 M_J$ companion is separated by 55 AU from a brown dwarf suggests that wide-binary stellar companions of mass $\approx 5 M_J$ may not be unusual. The same group has found that AB Pictoris has a $\approx 13 - 14 M_J$ companion separated by ≈ 270 AU. A Jupiter mass or larger object on a highly inclined orbit in the inner Oort cloud would most likely have formed as a small, distant binary-star like companion, e.g., by fragmentation during collapse or capture. We conclude that a model of a hypothetical wide-binary solar companion of mass $\approx 3 - 10 M_J$ orbiting at distances of $\approx 10,000$ AU is no less cosmogonically plausible than is the stellar impulse scenario.

Appendix A. Dynamics

We approximate the companion orbit as an invariant ellipse of mass and orbital parameters m_c, a_c, q_c, Q_c, i_c having orbit normal $\hat{\mathbf{n}}_c$. The heliocentric companion position is denoted by \mathbf{r}_c while the heliocentric Sedna position is \mathbf{r} . The barycentric solar location is

$$\mathbf{r}_\odot = -\frac{m_c}{M_\odot + \sum_p M_p + m_c} \mathbf{r}_c \equiv -\frac{m_c}{M_\odot + m_c} \mathbf{r}_c. \quad (A1)$$

Newton's equations of motion for the STNO are then

$$\ddot{\mathbf{r}} = -\ddot{\mathbf{r}}_\odot + \mathbf{g}_\odot + \sum_p \mathbf{g}_p + \mathbf{g}_c, \quad (A2)$$

where $\mathbf{g}_{\odot,p,c}$ are the gravitational fields at the STNO's location due to the Sun, the planets and the companion, respectively.

Further, we approximate the planetary perturbations by treating the planets as circular rings. In the limits $r_p \ll r \ll r_c$, we expand both the planetary and companion interactions. Thus

$$\begin{aligned} \mathbf{g}_\odot &= \nabla_{\mathbf{r}} \left(\frac{\mu_\odot}{r} \right) \\ \mathbf{g}_p &\approx \nabla_{\mathbf{r}} \left(\frac{\mu_p}{r} + \frac{\mu_p r_p^2}{4r^5} \left(r^2 - 3(\mathbf{r} \cdot \hat{\mathbf{n}}_p)^2 \right) \right) \end{aligned} \quad (A3)$$

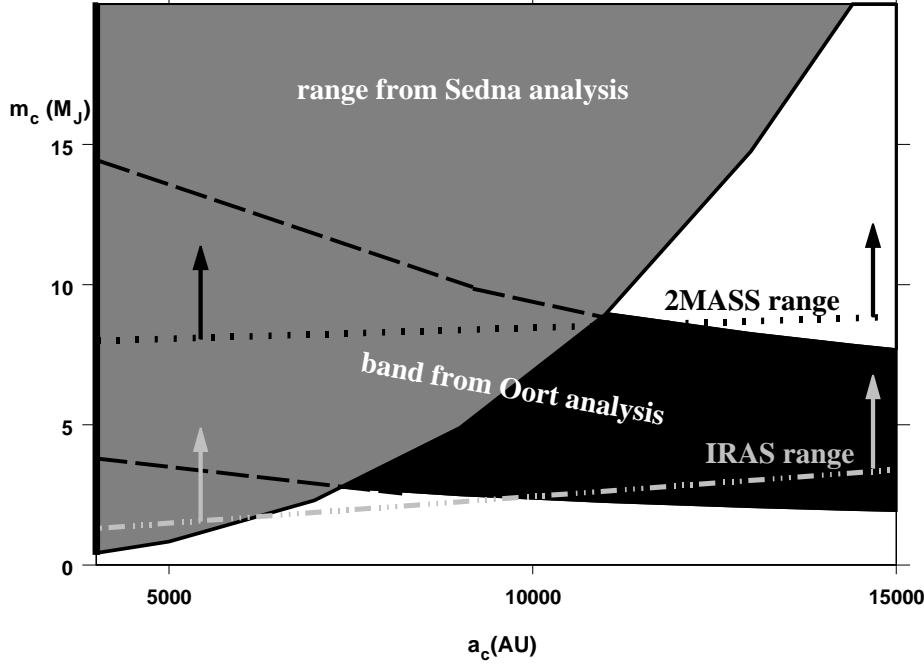


Figure 7. Assuming $e_c = 0.5$, we show the parameter ranges m_c , a_c where a solar companion could (i) detach and create a STNO during the epoch when γ_c was largest, (ii) produce the anomalous concentration of outer Oort cloud comets with the present epoch parameters and, (iii) be observed in the 2MASS and IRAS databases if, at present, $r_c = a_c$. Similar curves obtain for other values of e_c .

$$\mathbf{g}_c = \nabla_{\mathbf{r}} \left(\frac{\mu_c}{|\mathbf{r} - \mathbf{r}_c|} \right) \approx \nabla_{\mathbf{r}} \left(\frac{\mu_c \left(2\mathbf{r}_c \cdot \mathbf{r} r_c^2 + 3(\mathbf{r}_c \cdot \mathbf{r})^2 - r^2 r_c^2 \right)}{2r_c^5} \right).$$

Combining these results, we obtain

$$\begin{aligned} \ddot{\mathbf{r}} &\approx \nabla_{\mathbf{r}_c} \left(\frac{\mu_c}{r_c} \right) + \nabla_{\mathbf{r}} \left(\frac{\mu_o}{r} + \frac{\mathcal{I}_p \left(r^2 - 3(\mathbf{r} \cdot \hat{\mathbf{n}}_p)^2 \right)}{4r^5} + \frac{\mu_c \left(2\mathbf{r}_c \cdot \mathbf{r} r_c^2 + 3(\mathbf{r}_c \cdot \mathbf{r})^2 - r^2 r_c^2 \right)}{2r_c^5} \right) \\ &= \nabla_{\mathbf{r}} \left(\frac{\mu_o}{r} + \frac{\mathcal{I}_p \left(r^2 - 3(\mathbf{r} \cdot \hat{\mathbf{n}}_p)^2 \right)}{4r^5} + \frac{\mu_c \left(3(\mathbf{r}_c \cdot \mathbf{r})^2 - r^2 r_c^2 \right)}{2r_c^5} \right) \equiv \mathbf{a}_o + \mathbf{a}_p + \mathbf{a}_c, \quad (\text{A } 4) \end{aligned}$$

where $\mathcal{I}_p \equiv \sum_p \mu_p r_p^2$ and $\mu_o \equiv \mu_\odot + \sum_p \mu_p$.

We then construct the equations of motion for the scaled angular momentum vector and the eccentricity vector,

$$\mathbf{h} \equiv \frac{\mathbf{r} \times \dot{\mathbf{r}}}{\sqrt{\mu_o a}}, \quad \mathbf{e} \equiv \frac{\dot{\mathbf{r}} \times \mathbf{h}}{\sqrt{\mu_o/a}} - \hat{\mathbf{r}}, \quad (\text{A } 5)$$

which yields:

$$\dot{\mathbf{h}} = \frac{\mathbf{r} \times (\mathbf{a}_p + \mathbf{a}_c)}{\sqrt{\mu_o a}}, \quad \dot{\mathbf{e}} = \frac{\left((\mathbf{a}_p + \mathbf{a}_c) \times \mathbf{h} + \dot{\mathbf{r}} \times \dot{\mathbf{h}} \right)}{\sqrt{\mu_o/a}}. \quad (\text{A } 6)$$

Expressing the positions of the STNO and the companion in vector form

$$\mathbf{r} = \frac{a(1-e^2)}{1+e \cos f} \left(\hat{\mathbf{e}} \cos f + (\hat{\mathbf{h}} \times \hat{\mathbf{e}}) \sin f \right), \quad (\text{A } 7)$$

$$\mathbf{r}_c = \frac{a_c(1-e_c^2)}{1+e_c \cos f_c} \left(\hat{\mathbf{e}}_c \cos f_c + (\hat{\mathbf{n}}_c \times \hat{\mathbf{e}}_c) \sin f_c \right), \quad (\text{A } 8)$$

we sequentially perform secular averages over the short (STNO) orbital period and the long (companion) orbital period to obtain:

$$\langle \dot{\mathbf{h}} \rangle = \frac{2(\hat{\mathbf{n}}_p \cdot \mathbf{h}) \hat{\mathbf{n}}_p \times \mathbf{h}}{h^5 \tau_p} + \frac{5(\hat{\mathbf{n}}_c \cdot \mathbf{e}) \hat{\mathbf{n}}_c \times \mathbf{e} - (\hat{\mathbf{n}}_c \cdot \mathbf{h}) \hat{\mathbf{n}}_c \times \mathbf{h}}{\tau_c} \quad (\text{A } 9)$$

$$\begin{aligned} \langle \dot{\mathbf{e}} \rangle = & \frac{(h^2 - 3(\hat{\mathbf{n}}_p \cdot \mathbf{h})^2) \mathbf{h} \times \mathbf{e} - 2(\hat{\mathbf{n}}_p \cdot \mathbf{h}) (\hat{\mathbf{n}}_p \cdot (\mathbf{h} \times \mathbf{e})) \mathbf{h}}{h^7 \tau_p} + \\ & + \frac{\mathbf{h} \times \mathbf{e} + 4(\hat{\mathbf{n}}_c \cdot \mathbf{e}) \hat{\mathbf{n}}_c \times \mathbf{h} + (\hat{\mathbf{n}}_c \cdot (\mathbf{h} \times \mathbf{e})) \hat{\mathbf{n}}_c}{\tau_c}, \end{aligned} \quad (\text{A } 10)$$

where

$$\frac{1}{\tau_p} \equiv \frac{3\mathcal{I}_p}{8\sqrt{\mu_o a^7}} \xrightarrow{\text{Sedna}} \frac{1}{10 \text{ Gy}} \quad \text{and} \quad \frac{1}{\tau_c} \equiv \frac{3m_c}{4M_o} \sqrt{\frac{\mu_o a^3}{q_c^3 Q_c^3}} \equiv \frac{\gamma_c}{\tau_p}. \quad (\text{A } 11)$$

These analytic forms are obtained using *Mathematica* (Wolfram Research (2003)).

We see in Eq. A9 that the secular planetary interaction produces orbit normal precession around $\hat{\mathbf{n}}_p$, while a similar term in the secular companion interaction produces orbit normal precession around $\hat{\mathbf{n}}_c$. It is the term $\propto (\hat{\mathbf{n}}_c \cdot \mathbf{e}) \hat{\mathbf{n}}_c \times \mathbf{e}$ that dominates the nutation of \mathbf{h} and the changes in perihelion distances for large-eccentricity STNO. The analysis reproduces a well-known result: In the secular approximation, planetary perturbations alone do not change e (Goldreich (1965)).

The secularly averaged equations depend on the companion elements through the quantities $\hat{\mathbf{n}}_c$ and τ_c . There are several symmetries evident in the equations, such as their invariance when $\hat{\mathbf{n}}_c \rightarrow -\hat{\mathbf{n}}_c$, *i.e.*, $i_c \rightarrow \pi - i_c$, and their independence of the companion perihelion direction, $\hat{\mathbf{e}}_c$.

Orienting our axes as shown in figure 1, we see that the companion can be characterized by two parameters, γ_c and i_c , assumed to be constant here. Of course a wide-binary companion orbit is subject to perturbations from passing stars and the galactic tide. Therefore, these parameters essentially describe the epoch when companion interactions with the STNO are strongest, *i.e.*, when γ_c is largest. The galactic tide will change e_c and i_c , but changes are small for $a_c \lesssim 10,000$ AU. Osculations proceed through \gtrsim one half-cycle in 4.6 Gy when $a_c \gtrsim 20,000$ AU.

The STNO orbit is characterized by a secularly constant semimajor axis, a , and four variable elements i, ω, Ω and e . The six coupled equations for the components of \mathbf{e} and \mathbf{h} are restricted by the two conserved quantities, $\mathbf{h} \cdot \mathbf{e} = 0$ and $h^2 + e^2 = 1$, which serve as checks on our numerical solutions.

Acknowledgements

The authors gratefully acknowledge informative exchanges with Rodney Gomes. J.J.L. received support from NASA Planetary Geology and Geophysics Grant 344-30-50-01.

References

- Brown, M. E. Trujillo, C. & Rabinowicz, D. 2004, *ApJ* 617, 645
Burrows, A., Sudarsky, D., & Lunine, J. I. 2003, *ApJ* 596, 587
Chauvin, G. , *et al.* 2004, *A&A* 425(2) L29
Emel'yanenko, V. V., Asher, D. & Bailey, M. 2002, *MNRAS* 338(2), 443
Goldreich, P. 1965, *Rev. Geophys.* 4, 411
Gomes, R. S., Gallardo, T., Fernández, J. A. and Brunini, A. 2005, *CeMDA* 91, 109
Gomes, R. S., Matese, J. J., and Lissauer, J. J. 2006, *Icarus* (in press)
Matese, J. J., Whitman, P. G. & Whitmire, D. P. 1999, *Icarus* 141, 354
Matese, J. J., & Lissauer, J. J. 2002, *Proceedings of ACM2002* ESA SP-500 309
Morbidelli, A. & Levison, H. 2004, *AJ* 128, 2564
Wolfram Research 2003, *Mathematica* 5